Available online at www.sciencedirect.com

SciVerse ScienceDirect

Journal of the European Ceramic Society 32 (2012) 1643–1650

www.elsevier.com/locate/jeurceramsoc

# Effects of modified-process on the microstructure, internal bias field, and activation energy in CuO-doped NKN ceramics

Song-Ling Yang [a], Cheng-Shong Hong [b], Cheng-Che Tsai [c], Yi-Cheng Liou [d], Sheng-Yuan Chu [a,e,*]

[a] *Department of Electrical Engineering, National Cheng Kung University, Tainan 701, Taiwan, ROC*
[b] *Department of Electronic Engineering, National Kaohsiung Normal University, Kaohsiung County 824, Taiwan, ROC*
[c] *Department of Electronics Engineering and Computer Science, Tung-Fang Design University, Kaohsiung 82941, Taiwan ROC*
[d] *Department of Electronic Engineering, Kun Shan University, Tainan 71003, Taiwan, ROC*
[e] *Center for Micro/Nano Science and Technology and Research Center for Energy Technology and Strategy, National Cheng Kung University, Tainan 701, Taiwan, ROC*

Received 30 September 2011; received in revised form 2 December 2011; accepted 5 December 2011
Available online 15 January 2012

**Abstract**

In this study, $(Na_{0.5}K_{0.5})NbO_3 + xCuO$ (NKNC$x$, where $x = 0$–1 mol%) were separately prepared using the two-step calcination process (BO method) and a conventional mixed oxide method (MO method). The microstructure of NKNC$x$ ceramics prepared using the MO method exhibited obviously inhomogeneous microstructure. In contrast, the BO method improved the compositional homogeneity as well as the electrical properties. A high $Q_m$ value of 2100 was obtained for NKNC$x$ ceramics prepared using the BO method. The ceramics prepared using the BO method exhibited the formation of more oxygen vacancies, resulting in an increase in the internal bias field. The value for the activation energy of the samples supports the presence of oxygen vacancies. The bulk density, dielectric loss, $k_p$, $Q_m$, $d_{33}$ and $\varepsilon_{33}{}^T/\varepsilon_0$ of the NKNC$x$ ceramics prepared using the BO method were 4.488 g/cm$^3$, 0.15%, 41.5%, 2100, 95 pC/N and 280, respectively.
© 2011 Elsevier Ltd. All rights reserved.

*Keywords:* Two-step calcination process; Microstructure; Oxygen vacancies; Internal bias field; Activation energy

## 1. Introduction

Piezoelectric ceramics have been widely investigated because they can be used on piezoelectric actuators, ultrasonic motors, and piezoelectric transformers.[1,2] Lead zirconate titanate-based (PZT-based) ceramics are conventionally used materials, which exhibit excellent piezoelectric properties, such as high electromechanical coupling coefficient ($k_p$, $k_t$ and $k_{33}$), piezoelectric coefficient ($d_{33}$), dielectric constant ($\varepsilon_{33}$) and mechanical quality factor ($Q_m$).[3,4] However, high volatilization of PbO causes contamination during the sintering process and its toxicity is harmful to both human health and the environment. With increasing the environmental consciousness, the development of a lead-free material to replace the Pb-based ceramics is required. To meet such need, $(Bi_{1/2}M_{1/2})TiO_3$ (where M = Na, K; BMT) and (Na, K)$NbO_3$ (NKN) lead-free piezoelectric ceramics have been undergone rapidly development in the past decade because of their superior piezoelectric characteristics, especially in NKN-based systems. NKN ceramics have a perovskite structure with a high Curie temperature ($T_c \sim 420^\circ$) and a high electromechanical coupling coefficient. However, it is difficult to synthesize pure NKN as a dense ceramic at high sintering temperatures in air.[5] To overcome this problem, different methods including hot-pressing and spark plasma sintering (SPS) techniques have been used.[6,7] In addition, two different compound systems $LiBO_3$ (where B = Nb, Ta and Sb) and CuO-based compounds, have been added into NKN ceramics to improve the coupling coefficient and the mechanical quality factor, respectively.[8–13] However, most studies have achieved $Q_m$ values are between 1200 and 2000. To synthesize the samples of higher $Q_m$ values, process-modified methods may offer an alternative for the enhancement of piezoelectric characteristics.

In the 1980s, Swartz and Shrout reported a two-stage calcination method (columbite method) that depressed the pyrochlore

* Corresponding author. Tel.: +886 6 2757575x62381; fax: +886 6 2345482.
*E-mail address:* chusy@mail.ncku.edu.tw (S.-Y. Chu).

0955-2219/$ – see front matter © 2011 Elsevier Ltd. All rights reserved.
doi:10.1016/j.jeurceramsoc.2011.12.008

phase and thus improved the electrical properties.[14] Later, Kim et al. proposed using the two-step calcination process (BO method) to prepare PZT ceramics and thus improved the homogeneous microstructure and piezoelectric properties.[15] Moreover, some experimental results have been reported for the dielectric, piezoelectric and dynamic aging properties of PZT-based system synthesized by the BO method. These results show superior electrical properties due to the fine-grain and homogeneous microstructure of ceramics.[16–18] Similarly, this method has also used for the preparation of lead-free piezoelectric ceramics. Wang et al. reported the initial mixing and calcination of $Nb_2O_5$ and $Ta_2O_5$ to form a B-site oxide precursor, and the subsequent addition of $Li_2CO_3$, $K_2CO_3$, $Na_2CO_3$ powders into the solid solution oxide of $Nb_2O_5$ and $Ta_2O_5$, to form (Li, K, Na)(Nb, Ta)$O_3$ ceramics. This two-step calcination process thus improved the compositional homogeneity and piezoelectric properties of the samples.[19] It is believed that the BO method is a more comprehensive and generic technology, which allows superior behaviors, than the conventional mixed oxide method (MO), or the columbite precursor method.[20]

Past studies have shown that the oxygen vacancy plays an important role in "hard" piezoelectric ceramics. The $Q_m$ value of samples is significantly affected by the concentration of oxygen vacancies, which prevent the domain walls from moving. However, it is not easy to explain the concentration of oxygen vacancies in the ceramics. In this study, the ceramics were prepared by the two-step calcination process (BO method) and conventional mixed oxide method (MO method) and the effect of the different methods on the physical and electrical properties of the ceramics was investigated. An internal bias field and Cole–Cole plots were used to illustrate the concentrations and presence of oxygen vacancies in the samples. A high $Q_m$ value of over 2000 was obtained for CuO-doped NKN ceramics prepared using the BO method.

## 2. Experimental procedures

Ceramics composed of $(Na_{0.5}K_{0.5})NbO_3 + x$CuO (NKNC$x$, where $x$ = 0–1 mol%) were prepared using the MO and BO methods, with pure oxides of $Na_2CO_3$, $K_2CO_3$, $Nb_2O_5$ and CuO powders (>99% purity) as the starting materials. For the MO method, $Na_2CO_3$, $K_2CO_3$ and $Nb_2O_5$ powders were ball-milled in a polyethylene jar with $ZrO_2$ balls, for 24 h using ethanol as the medium. Then, the slurries were dried and calcined twice (to enhance the compositional uniformity), at 900 °C for 5 h, in air. After calcination, CuO was doped into the NKN powders and the NKN-CuO powders were then ball-milled for another 24 h. For the BO method, $Nb_2O_5$ and CuO powders were firstly calcined at 1000 °C for 5 h twice as a B-site precursor. Then the $Na_2CO_3$, $K_2CO_3$ and (Nb, Cu) precursors were weighed according to the stoichiometric formula and ball-milled together for 24 h. After drying, the powder was calcined at 900 °C for 5 h twice in air and then re-milled for 24 h. These two powder batches were separately mixed with PVA aqueous solution and then pressed into a disk (12 mm in diameter and 1.2 mm in thickness) at a pressure of 100 MPa. All the specimens were sintered at 1100 °C for 2 h, in air, at a heating rate of 5 °C/min.

The crystallographic profile was determined by X-ray diffraction (XRD) using $CuK_\alpha$ ($\lambda$ = 0.15406 nm) radiation with a Rigaku MultiFlex X-ray diffractometer operated at 30 kV and 20 mA. In order to confirm the exact diffracted angles, silicon powders were used for calibration. The microstructure was observed using scanning electron microscopy (SEM) with a Hitachi S-4100 microscope. Bulk densities were measured using the Archimedes method with distilled water as the medium. The piezoelectric properties were measured with an HP 4294A precision impedance analyzer and an APC P/N 90-2030 $d_{33}$ meter. To measure the electrical properties, silver paste was painted on both sides of the samples to form electrodes. The samples were then fired at 800 °C for 30 min and then poled by a DC field (30 kV/cm) at 125 °C for 30 min, in a silicone oil bath. The electromechanical coupling factor in planar ($k_p$) mode and the mechanical quality factor ($Q_m$) were calculated using the resonance–anti-resonance method.[11]

$$\frac{1}{k_p^2} = 0.395 \times \frac{f_r}{f_a - f_r} + 0.574 \quad (1)$$

$$Q_m = \frac{1}{2\pi f_r R_z C_s [1 - (f_r/f_a)^2]} \quad (2)$$

where $f_r$ is the resonance frequency, $f_a$ is the anti-resonance frequency, $R_z$ is the resonance impedance, and $C_s$ is the capacitance at 1 kHz.

Both the real and imaginary parts of the impedances of the samples were measured at temperatures from 723 K to 1023 K and frequencies from 100 Hz to 100 MHz using an HP 4294A precision impedance analyzer. Ferroelectric hysteresis loops ($P$–$E$) were obtained in an AC of 3–4 kV at 60 Hz using a modified Sawyer–Tower circuit.[21]

## 3. Results and discussion

In the present paper, it is important to obtain the precursors of pre-reacted $Nb_2O_5$ and CuO. Therefore, XRD and EDS analysis were used to confirm the reaction of $Nb_2O_5$ and CuO powders. However, $Nb_2O_5$ with CuO doping and $Nb_2O_5$ powders showed the same XRD patterns because of a low concentration of CuO doping (<1 mol%). The B-site oxide precursors ($Nb_2O_5$ with CuO doping) could be still demonstrated by EDS analysis, as shown in Fig. 1. Fig. 1 shows it can be observed that $Nb_2O_5$ powders contain Cu atoms after the $Nb_2O_5$ and CuO powders are calcined at 1000 °C for 5 h. Therefore, the B-site oxide precursors are definitely obtained from $Nb_2O_5$ and CuO powders after calcining. Fig. 2 shows the XRD profile of NKNC$x$ ceramics prepared using the BO method. All the samples of NKNC$x$ ceramics have a perovskite structure but no secondary phase, implying that the BO method does not cause any significant change in the structure of CuO-doped NKN ceramics. As seen in Fig. 2, the diffracted angles shift to lower angles, as $x \geq 0.25$ mol%. This is because the Cu ionic radius is close to the Nb ionic radius so $Nb^{5+}$ ions are substituted by $Cu^{2+}$ ions. Moreover, the variation in the diffracted angles in NKNC$x$ ceramics

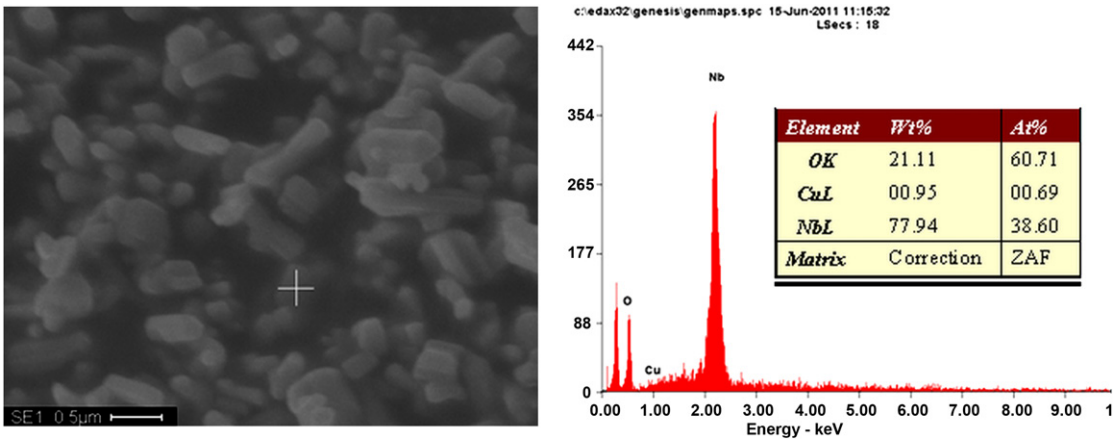


Fig. 1. SEM and EDS images of CuO-doped $Nb_2O_5$ powders calcined at 1000 °C for 5 h.

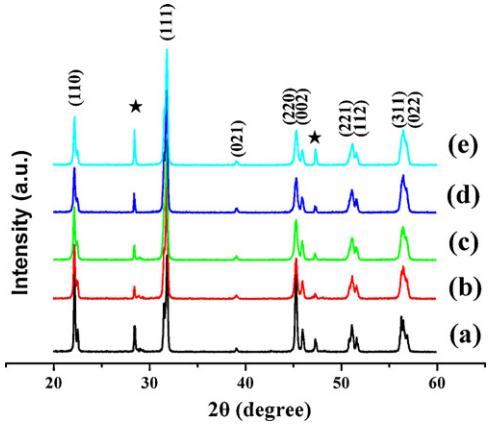


Fig. 2. XRD profiles of NKNC*x* ceramics prepared using the BO method. (a) 0 mol% CuO, (b) 0.25 mol% CuO, (c) 0.5 mol% CuO, (d) 0.75 mol% CuO, and (e) 1 mol% CuO (⋆: Si powder).

occurs because the ionic radius of $Cu^{2+}$ (0.73 Å) exceeds that of $Nb^{5+}$ (0.64 Å), which leads to an increase in the lattice constant and an expansion of the lattice volume. According to Bragg's law, $\lambda = 2d \sin\theta$, and since NKN ceramics have an orthorhombic structure at room temperature (an orthorhombic structure was also observed in the split of (2 2 0) and (0 0 2) of XRD profiles), $(1/d^2) = (h^2/a^2) + (k^2/b^2) + (l^2/c^2)$ was obtained. These two equations above indicate that the lattice constant is inversely proportional to the diffracted angle. Therefore, the diffracted angles shift to lower angles, as the lattice constant increases. CuO-doped NKN ceramics using the MO method also exhibited a similar XRD profile (XRD profiles are not shown in this paper).

SEM images of NKNC*x* powders after calcination at 900 °C for 5 h, using the MO and BO methods, are shown in Fig. 3. The SEM image of CuO-doped NKN powder obtained using the BO method also shows smaller grain size and much better compositional homogeneity, giving samples with a fine-grain structure, after sintering. The microstructures of NKNC*x* ceramics prepared using MO and BO methods are shown in Fig. 4. Many researchers have reported that it is difficult to obtain dense NKN ceramics at high sintering temperatures in air. As seen in Fig. 4(a), pure NKN ceramics with some pores were obtained by this study. When CuO dopants were doped into NKN ceramics (see Fig. 4(b)), the samples showed a dense grain structure because copper oxide acts as a sintering aid and facilitates the movement of grains. However, the liquid phase is not obvious in Fig. 4(b), because the liquid phase formed by CuO has a high solubility during the sintering process. Hence, its presence in NKN ceramics is not permanent and it disappears along with sintering.[22,23] The two-step calcination process was first used to prepare PZT ceramics, in order to enhance their density and the piezoelectric properties, owing to the fine-grain structure and better homogeneity.[15] The microstructures of NKNC*x*

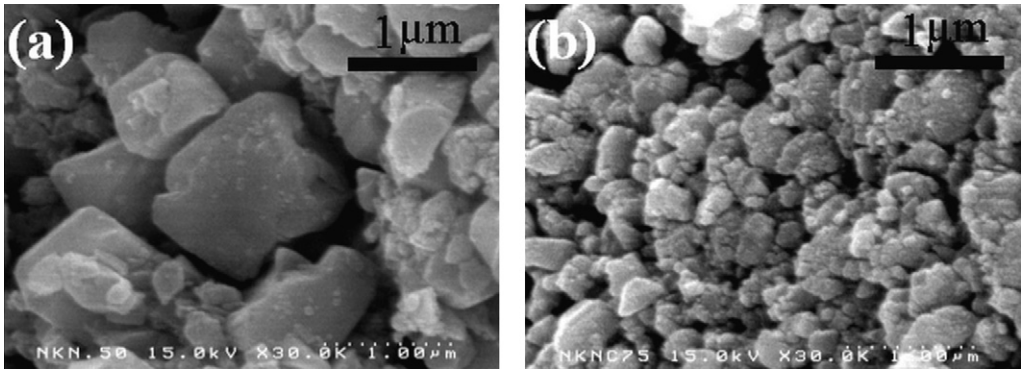


Fig. 3. SEM images of CuO-doped NKN powders after calcination at 900 °C for 5 h using (a) MO and (b) BO methods.

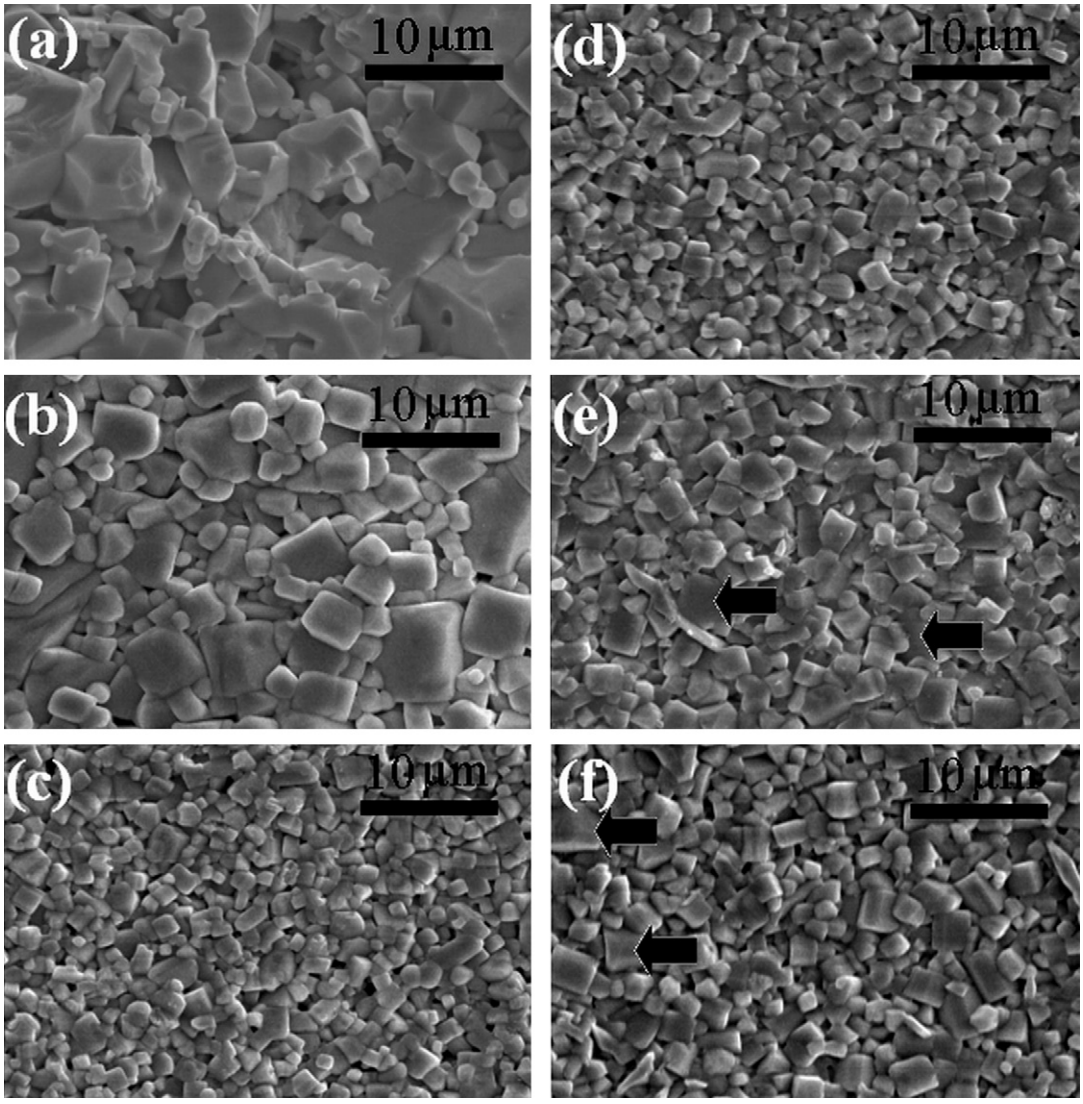


Fig. 4. SEM images of the surface microstructures of NKNC*x* ceramics prepared using MO and BO methods. (a) 0 mol% CuO and (b) 0.5 mol% CuO using the MO method, and (c) 0.25 mol% CuO, (d) 0.5 mol% CuO, (e) 0.75 mol% CuO, and (f) 1 mol% CuO using the BO method.

ceramics prepared using the BO method exhibited a pronounced change, showing a more homogeneous microstructure compared than that of NKNC*x* ceramics synthesized by the MO method (as compared Fig. 4(b)–(f)). The distribution of grain size for NKNC*x* ceramics prepared using MO and BO methods are shown in Fig. 5 (the number of grain is more than 200 in the calculation of grain size distribution). NKNC*x* ceramics prepared using the BO method exhibit a range of grain sizes between 0.5

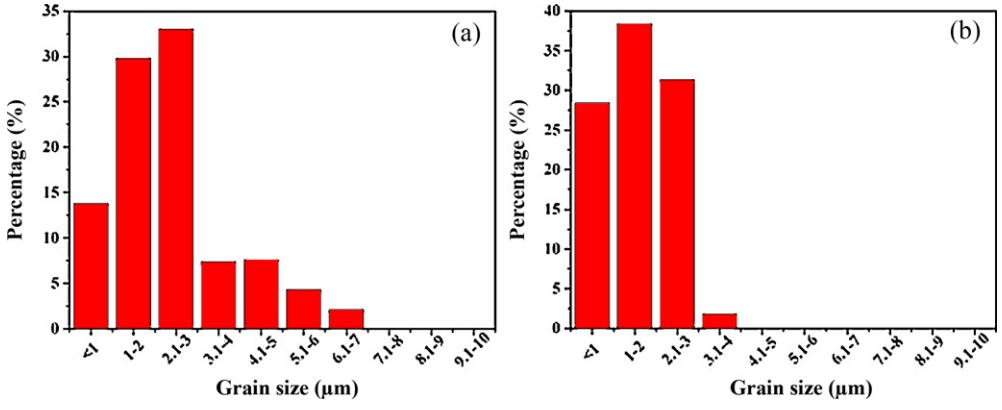


Fig. 5. The range of grain size for NKNC*x* ceramics prepared using (a) MO and (b) BO methods at $x = 0.5$ mol% (calculated from Fig. 4(b) and (d)).

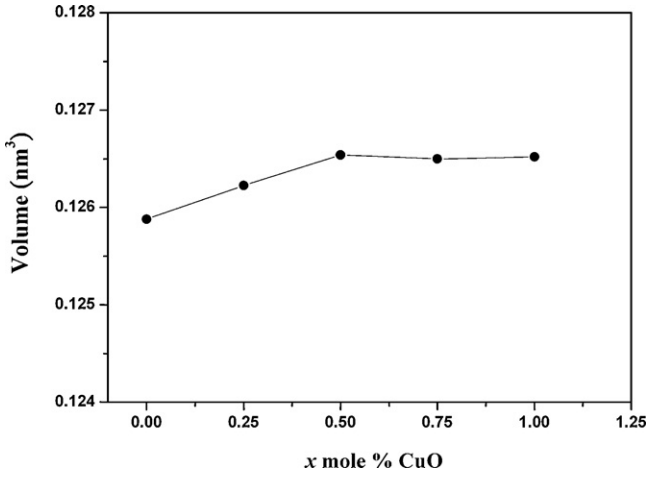


Fig. 6. Lattice volumes of NKNC$x$ ceramics were calculated from the plane index of XRD profiles of samples using the BO method.

and 4 μm, which is smaller than that for grain sizes between 0.5 and 7 μm, obtained for ceramics prepared using the MO method. This result illustrates that NKNC$x$ ceramics with more homogeneous microstructure are obtained using the BO method. In addition, the grain size of NKNC$x$ ceramics prepared using the BO method is smaller than that of ceramics synthesized by the MO method. For the BO method, it is understood that both CuO and $Nb_2O_5$ are pre-reacted and that CuO has been incorporated into $Nb_2O_5$ (see in Fig. 1). Therefore, CuO dopants cannot form a liquid phase, which results in the production of NKN ceramics with small grain size by the BO method. The compositional homogeneity is also related to the thermodynamic stability and diffusion kinetics. Wang et al. reported that reducing the diffusion distance of the compositional elements (by mechanical methods) or depressing the thermodynamically preferable grouping of A- and B-site (using the BO method) are crucially important to improving the homogeneity of ceramics.[19] In addition, the oxide mixture is not properly processed, which results in both volumetric expansion and morphological transformations leading to the formation of ceramics with inhomogeneous densification.[15] In this study, NKNC$x$ ceramics with homogeneous structure were obtained using the BO method.

As $x \geq 0.75$ mol%, some grains of NKNC$x$ ceramics prepared using the BO method become suddenly greater (arrowheads), as seen in Fig. 4(e) and (f), suggesting that the solubility limit of CuO incorporated into $Nb_2O_5$ reaches saturation. Consequently, the residual CuO react with $K_2CO_3$ and $Nb_2O_5$ to form a liquid phase, which improves the densification of NKNC$x$ ceramics. However, the secondary phase with copper oxide was not detected in XRD profiles, owing to the resolution of the X-ray diffraction. The solubility limit of the CuO incorporated into the Nb sites is still demonstrated, as seen in Fig. 6. The lattice volumes of NKNC$x$ ceramics prepared using the BO method is shown in Fig. 6. As can be seen, the lattice volumes increases as the amount of CuO doping increases, reaching saturation at a value of $x$ between 0.5 and 0.75 mol%. Excessive CuO remains as $x \geq 0.75$ mol%, causing the formation of the liquid phase. In order to confirm the formation of the liquid phase, EDS

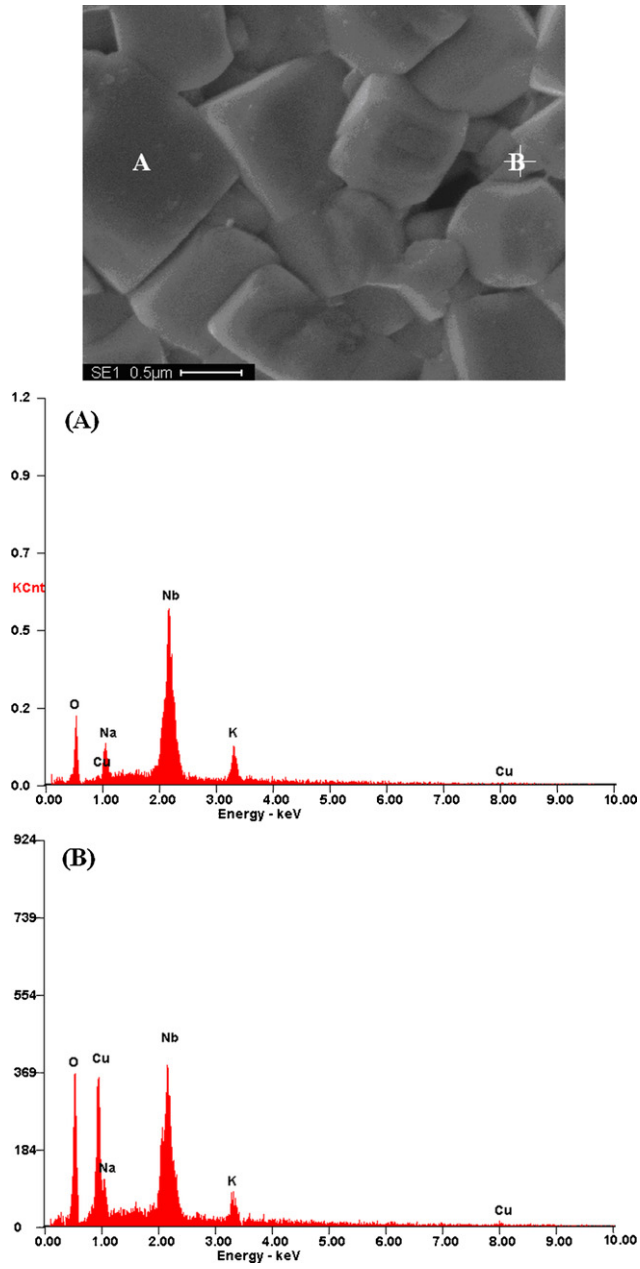


Fig. 7. SEM and EDS images of NKN + 0.75 mol% CuO ceramics prepared using the BO method.

analysis of NKNC$x$ ceramics prepared using the BO method was performed and the results are shown in Fig. 7. As can be seen, the morphology of the NKN ceramics exhibited square grains (spot A), and the formation of a compound (K, Nb, Cu) liquid phase in the grain boundary (spot B). Such observations again verify that the use of excessive CuO in the BO method causes $K_2CO_3$ and $Nb_2O_5$ to form a liquid phase, as $x \geq 0.5$ mol%. From these results, it can be seen that when CuO dopants are doped into NKN ceramics, Cu ions replace Nb ions, because the diffracted angles shift to lower angles under changes in lattice volumes, as seen in XRD profiles ($x = 0$–$0.5$ mol%). Moreover, the solubility limit for CuO doping occurs at $x = 0.5$ mol% and further doping of CuO contributes to densification of the samples, because the residual CuO and $K_2CO_3$, $Nb_2O_5$ form a liquid

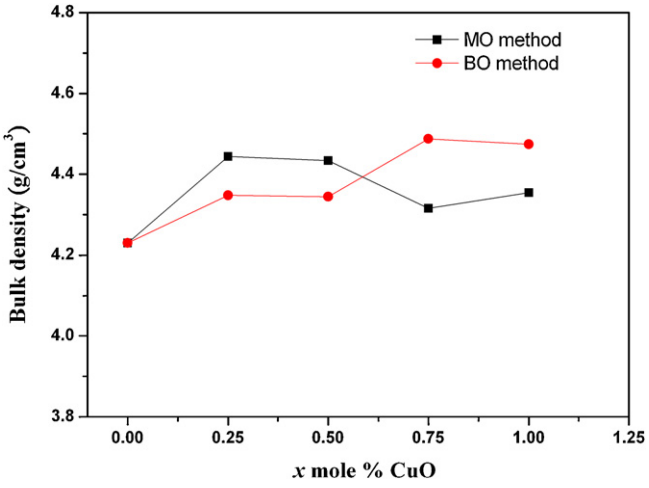


Fig. 8. Bulk density of the NKNC*x* ceramics prepared using MO and BO methods.

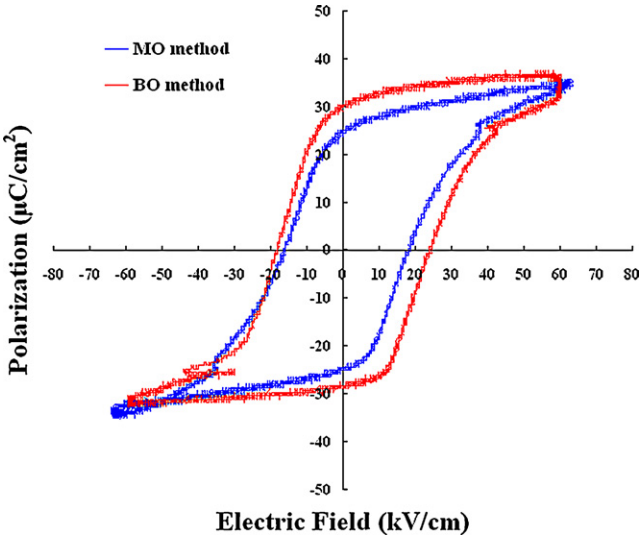


Fig. 9. P-E hysteresis loops of CuO-doped NKN ceramics prepared using MO and BO method.

phase. Fig. 8 shows the bulk density of NKNC*x* ceramics prepared using the MO and BO methods. The density of NKNC*x* ceramics prepared using the MO method increases as the amount of CuO doping increases and then drops at $x = 0.75$ mol%. The maximum density of 4.444 g/cm$^3$ is obtained in NKNC*x* ceramics synthesized by the MO method. However, the greater bulk density value of 4.488 g/cm$^3$ was obtained when using the BO method. This is probably because the microstructure of NKNC*x* ceramics prepared using the BO method exhibits a homogeneous microstructure. In general, compositional homogeneity with small-grain structure facilitates the formation of dense ceramics, because pores are easily formed in the inhomogeneous microstructure of ceramics. Therefore, the maximum density of NKNC*x* ceramics prepared using the BO method is higher than that of those prepared using the MO method. In Fig. 8, the density of NKNC*x* ceramics synthesized by the BO method shows two obvious changes at $x = 0$–0.25 mol% and $x = 0.5$–0.75 mol%. Firstly, at values of $x$ between 0 mol% and 0.25 mol%, pure NKN ceramics exhibit an inhomogeneous structure and many pores, which lead to a lower density. When CuO dopants are doped into the NKN ceramics, the bulk density increases, because of the compositional homogeneity (see Fig. 4(c)). Secondly, at values of $x$ between 0.5 mol% and 0.75 mol%, the maximum density of NKNC*x* ceramics synthesized by the BO method is obtained at $x = 0.75$ mol%. The higher density is not only the result of a homogeneous microstructure, but the liquid phase also contributes to the formation of a dense ceramic. As seen in the SEM images, the liquid phase is formed when the amount of CuO doping reaches 0.75 mol% or above, leading to a decrease in the number of pores in the NKNC*x* ceramics. The optimum amounts of CuO doping for NKN ceramics prepared using the MO method and BO method were 0.5 mol% and 0.75 mol%, respectively, due to the different reaction mechanisms.

The piezoelectric characteristics of NKNC*x* ceramics synthesized by the MO and BO methods are listed in Table 1. NKNC*x* ceramics exhibit a higher $Q_m$ value than pure NKN ceramics ($Q_m$: 67), because $Nb^{5+}$ ions are substituted by $Cu^{2+}$ ions and induce the oxygen vacancies. Many studies have reported that the formation of oxygen vacancies improves the $Q_m$ value because oxygen vacancies prevent domain walls from moving, resulting in "hard" piezoelectric materials.[24–26] $Q_m$ values of over 2000 in NKN-based ceramics are seldom encountered. However, a $Q_m$ value of 2100 in NKNC*x* ceramics prepared using the BO method was obtained. The presence and concentration of oxygen vacancies are important for "hard" piezoelectric ceramics with a high $Q_m$ value. In order to define the relationships between $Q_m$ and oxygen vacancy, the internal bias field ($E_i$) and activation energy in the ceramics prepared using MO and BO methods were calculated from P-E hysteresis loops and Cole–Cole plots, respectively. Fig. 9 shows the P-E hysteresis loops for CuO-doped NKN ceramics prepared using MO and BO methods. The built-in internal bias field causes the P-E hysteresis loops to be asymmetrical. The $E_i$ values of CuO-doped NKN ceramics prepared using MO and BO methods were calculated from the P-E hysteresis loops and are shown in Table 2. The $E_i$ value for CuO-doped NKN ceramics prepared using the MO

Table 1
Piezoelectric characteristics of CuO-doped NKN ceramics prepared using MO and BO methods.

| CuO-doped NKN ceramics | Density (g/cm$^3$) | $k_p$ | $Q_m$ | $\varepsilon_{33}{}^T/\varepsilon_0$ | tan $\delta$ (%) |
|---|---|---|---|---|---|
| NKN + 0.5 mol% CuO (MO method) | 4.434 | 0.396 | 1685 | 231 | 0.74 |
| NKN + 0.75 mol% CuO (MO method) | 4.316 | 0.343 | 1765 | 228 | 0.86 |
| NKN + 0.5 mol% CuO (BO method) | 4.345 | 0.41 | 1147 | 276 | 0.56 |
| NKN + 0.75 mol% CuO (BO method) | 4.488 | 0.415 | 2100 | 280 | 0.15 |

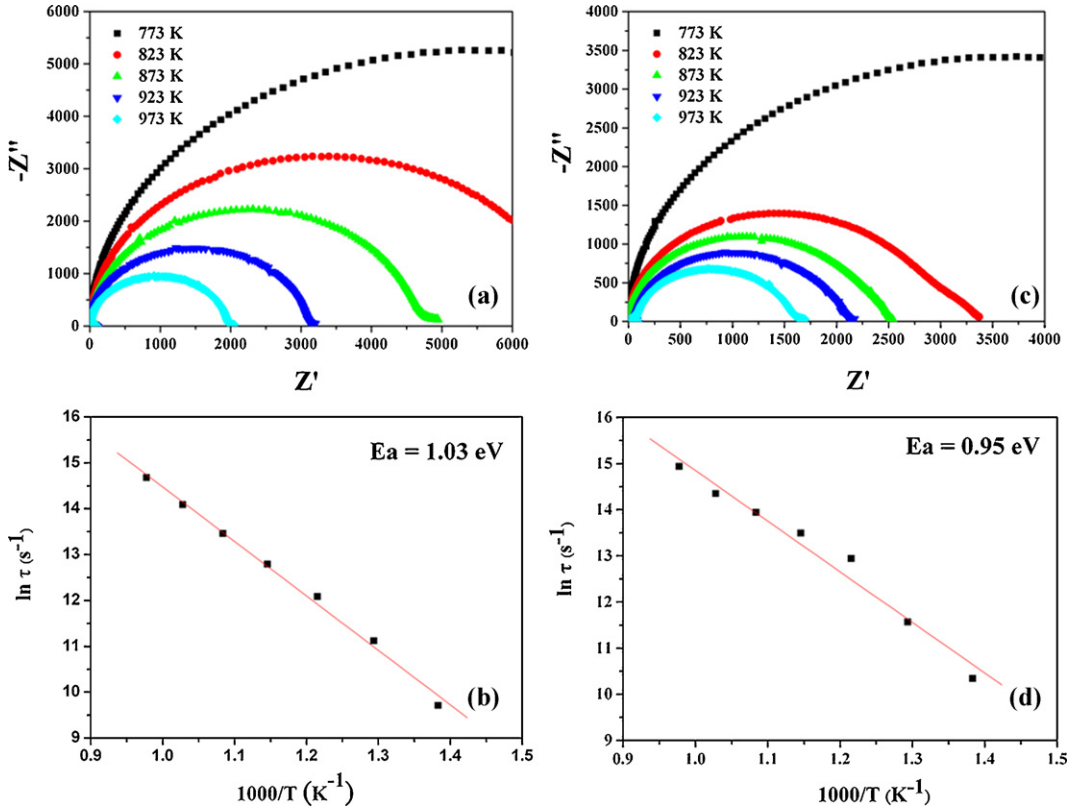


Fig. 10. Complex impedances and relaxation frequency of CuO-doped NKN ceramics prepared using (a) and (c) MO and (b) and (d) BO methods at different temperatures. The red line is a linear fit to Eq. (3). (For interpretation of the references to color in this figure legend, the reader is referred to the web version of the article.)

method is 1.45 kV/cm. However, the ceramics prepared using the BO method have a greater $E_i$ value (3.5 kV/cm), corresponding to a higher $Q_m$ value (2100) than samples prepared using the MO method. $Q_m$ is proportional to $E_i$, because the internal bias field reduces hysteresis loss, especially by preventing the motion of domain walls.[27] In addition, the $E_i$ value is affected by the concentrations of oxygen vacancies. The formation of more oxygen vacancies induces a greater $E_i$ value and thus increases the $Q_m$ value. In this study, the ceramics prepared using the BO method had a greater $E_i$ value, as the in the number of oxygen vacancies increased. Therefore, a higher $Q_m$ value was obtained for the ceramics prepared using the BO method. On the other hand, the activation energy also explains the presence of oxygen vacancies in CuO-doped NKN ceramics. Fig. 10(a) and (b) shows the Cole–Cole plots for CuO-doped NKN ceramics prepared using MO and BO methods. The activation energies are calculated from the relaxation frequency ($\omega$) at the apex of the Cole–Cole semicircle of the CuO-doped NKN ceramics and satisfy the condition, $\omega RC = 1$ ($\omega = 1/\tau$). The relaxation frequencies were plotted as a function reciprocal temperature for CuO-doped NKN ceramics in Arrhenius format as[28]:

$$\omega = \omega_0 \quad \exp\left(\frac{-E_a}{K_B T}\right) \tag{3}$$

where $\omega_0$ is the pre-exponential factor, $E_a$ is the activation energy of relaxation, $K_B$ is the Boltzmann constant and $T$ is the absolute temperature. The activation energy is obtained from the gradient of ln($\omega$) versus $1/T$ in Fig. 10(c) and (d), using Eq. (3). The activation energies of CuO-doped NKN ceramics prepared using MO and BO methods are 1.03 eV and 0.95 eV, respectively. Islam reported that the activation energy for oxygen vacancy migration is around 1 eV, by performing a computational simulation of ionic transport in perovskite oxides.[29] Consequently, the presence of oxygen vacancies was verified in CuO-doped NKN ceramics. The activation energies of samples vary according to the concentration and type of oxygen vacancy.[28] The ceramics prepared using MO and BO methods produce the different concentrations of oxygen vacancies, which caused the different activation energies for the samples. The ceramics prepared using the BO method have a greater number of oxygen vacancies, leading to a lower activation energy than that of those prepared using the MO method. Therefore, a high $Q_m$ value is obtained for CuO-doped NKN ceramics prepared using the BO method. In this study, the $Q_m$ and ${\varepsilon_{33}}^T/\varepsilon_0$ values for NKNC$x$ ceramics prepared using the BO method were improved by 25% and 21%, respectively, in comparison with those using the MO method. There are three possible reasons for this. Firstly, NKNC$x$ ceramics

Table 2
$Q_m$ value and internal bias field of the CuO-doped NKN ceramics prepared using MO and BO methods.

| Process | $Q_m$ | $E_i$ (kV/cm) |
|---|---|---|
| NKN + 0.5 mol% CuO (MO method) | 1685 | 1.15 |
| NKN + 0.75 mol% CuO (BO method) | 2100 | 3.50 |

synthesized by the BO method exhibit a homogeneous microstructure; both Pb-based and lead-free piezoelectric ceramics with homogeneous microstructure exhibited better piezoelectric properties in previous studies.[15,19] Secondly, the precursor of pre-reacted CuO and $Nb_2O_5$ causes the Cu ions to occupy the Nb sites more easily in NKNC*x* ceramics, thus promoting the formation of oxygen vacancies and increasing the $Q_m$ value when using the BO method. Finally, the effect of oxygen vacancies on the $Q_m$ value reaches a limit at $x = 0.5$ mol% (the solubility limit of Cu ions incorporated into the B-site is reached) and the $Q_m$ value then increases at $x = 0.75$ mol%, because the bulk density is enhanced by the liquid phase when using the BO method (see Figs. 7 and 8). Ceramics of higher density often exhibit better electrical properties. In this study, excellent piezoelectric properties were obtained using the BO method. In addition, the BO method improved the microstructure and electrical properties of not only "soft",[19] but also "hard" piezoelectric materials.

## 4. Conclusions

CuO-doped NKN ceramics synthesized by the BO method exhibited greater compositional homogeneity than samples prepared by the MO method. The expansion of the lattice volumes in NKNC*x* ceramics changes because the Nb sites are occupied by Cu ions. For the NKNC*x* ceramics prepared using the BO method, a liquid phase is formed as $x > 0.5$ mol%, as the residual CuO dopants are introduced, leading to an improvement in the bulk density and electrical properties. The ceramics prepared using the BO method exhibit a higher $Q_m$ value than those prepared using the MO method, because of the formation of more oxygen vacancies. In addition, both internal bias field and activation energy verified the formation and concentrations of CuO-doped NKN ceramics prepared using MO and BO methods. The mechanical quality factor, $Q_m$, and dielectric constant, $\varepsilon_{33}{}^{T}/\varepsilon_0$, of this system were increased by 21% and 25%, respectively, when using the BO method was used.

## Acknowledgments

We gratefully acknowledge the financial support from the Bureau of Energy, Ministry of Economic Affairs, Taiwan (Grant numbers: NSC 99-ET-006-008-ET, and 100-ET-E-006-003-ET). We also appreciate a native English language editing agency, K.T. Li Foundation for the Development of Science and Technology, for the help to polish our article.

## References

1. Moulson AJ, Herbert JM. *Electroceramics*. 2nd ed. New York: John Wiley and Sons; 2003.
2. Uchino K. *Piezoelectric Actuator and Ultrasonic Motors*. Massachusetts: Kluwer Academic Publisher; 1996.
3. Weston TB, Webster AH, Mcnamara VM. Lead zirconate–lead titanate piezoelectric ceramics with iron oxide additions. *J Am Ceram Soc* 1969;**52**:253–7.
4. Kondo M, Hida M, Tsukada M, Kurihara K, Kamehara N. Piezoelectric properties of $Pb(Ni_{1/3},Nb_{2/3})O_3$–$PbTiO_3$–$PbZrO_3$ ceramics. *Jpn J Appl Phys* 1997;**36**:6043–5.
5. Guo Y, Kakimoto K, Ohsato H. Dielectric and piezoelectric properties of lead-free $(Na_{0.5}K_{0.5})NbO_3$–$SrTiO_3$ ceramics. *Solid State Commun* 2004;**129**:279–84.
6. Haertling GH. Properties of hot-pressed ferroelectric alkali niobate ceramics. *J Am Ceram Soc* 1967;**50**:329–30.
7. Wang R, Xie R, Sekiya T, Shimojo Y, Akimune Y, Hirosaki N, Itoh M. Piezoelectric properties of spark-plasma-sintered $(Na_{0.5}K_{0.5})NbO_3$–$PbTiO_3$ ceramics. *Jpn J Appl Phys* 2002;**41**:7119–22.
8. Yang Z, Chang Y, Liu B, Wei L. Effects of composition on phase structure, microstructure and electrical properties of $(K_{0.5}Na_{0.5})NbO_3$–$LiSbO_3$ ceramics. *Mater Sci Eng A* 2006;**432**:292–8.
9. Guo Y, Kakimoto K, Ohsato H. Phase transitional behavior and piezoelectric properties of $(Na_{0.5}K_{0.5})NbO_3$–$LiNbO_3$ ceramics. *Appl Phys Lett* 2004;**85**:4121–3.
10. Guo Y, Kakimoto K, Ohsato H. $(Na_{0.5}K_{0.5})NbO_3$–$LiTaO_3$ lead-free piezoelectric ceramics. *Mater Lett* 2005;**59**:241–4.
11. Matsubara M, Yamaguchi T, Sakamoto W, Kikuta K, Yogo T, Hirano S. Processing and piezoelectric properties of lead-free (K,Na)(Nb,Ta)$O_3$ ceramics. *J Am Ceram Soc* 2005;**88**:1190–6.
12. Matsubara M, Kikuta K, Hirano S. Piezoelectric properties of $(K_{0.5}Na_{0.5})(Nb_{1-x}Ta_x)O_3$–$K_{5.4}CuTa_{10}O_{29}$ ceramics. *J Appl Phys* 2005;**97**:114105.
13. Lin D, Kwok KW, Chan HLW. Piezoelectric and ferroelectric properties of Cu-doped $K_{0.5}Na_{0.5}NbO_3$ lead-free ceramics. *J Phys D: Appl Phys* 2008;**41**:045401.
14. Swartz SL, Shrout TR. Fabrication of perovskite lead magnesium niobate. *Mater Res Bull* 1982;**17**:1245–50.
15. Kim S, Lee GS, Shrout TR. Fabrication of fine-grain piezoelectric ceramics using reactive calcination. *J Mater Sci* 1991;**26**:4411–5.
16. Robert G, Maeder ND, Damianovic D, Setter N. Synthesis of lead nickel niobate–lead zirconate titanate solid solutions by a B-site precursor method. *J Am Ceram Soc* 2001;**84**:2860–72.
17. Bove T, Wolny W, Ringgaard E, Pedersen A. New piezoceramic PZT–PNN material for medical diagnostics applications. *J Eur Ceram Soc* 2001;**21**:1469–72.
18. Tsai CC, Chu SY, Liang CK. Low-temperature sintered PMnN-PZT based ceramics using the B-site oxide precursor method for therapeutic transducers. *J Alloy Compd* 2009;**478**:516–22.
19. Wang Y, Damjanovic D, Klein N, Hollenstein E, SetterN. Compositional inhomogeneity in Li- and Ta-modified (K, Na)$NbO_3$ ceramics. *J Am Ceram Soc* 2007;**90**:3485–9.
20. Fang B, Shan Y, Tezuka K, Imoto H. Reduction of dielectric losses in $Pb(Fe_{1/2}Nb_{1/2})O_3$-based ferroelectric ceramics. *Jpn J Appl Phys* 2005;**44**:5035–9.
21. Sawyer CB, Tower CH. Rochelle as a dielectric. *Phys Rev* 1930;**35**:269–75.
22. Park HY, Choi JY, Choi MK, Cho KH, Nahm S, Lee HG, Kang HW. Effect of CuO on the sintering temperature and piezoelectric properties of $(Na_{0.5}K_{0.5})NbO_3$ lead-free piezoelectric ceramics. *J Am Ceram Soc* 2008;**91**:2374–7.
23. German RM. Transient liquids. In: *Liquid Phase Sintering.* 1st edition New York: Plenum Press; 1985. p. 164.
24. Hou YD, Zhu MK, Gao F, Wang H, Wang B, Yan H, Tian CS. Effect of $MnO_2$ addition on the structure and electrical properties of $Pb(Zn_{1/3}Nb_{2/3})_{0.2}(Zr_{0.5}Ti_{0.5})_{0.8}O_3$ ceramics. *J Am Ceram Soc* 2004;**87**:847–50.
25. Toshio K, Toshimasa S, Takaaki T, Masaki D. Effects of manganese addition on piezoelectric properties of $Pb(Zr_{0.5}Ti_{0.5})O_3$. *Jpn J Appl Phys* 1992;**31**:3058–60.
26. Lee SM, Lee SH, Yoon CB, Kim HE, Lee KW. Low-temperature sintering of $MnO_2$-doped PZT–PZN piezoelectric ceramics. *J Electroceram* 2007;**18**:311–5.
27. Takahashi S. Internal bBias field effects in lead zirconate–titanate ceramics doped with multiple impurities. *Jpn J Appl Phys* 1981;**20**:95–101.
28. Liu L, Fan H, Fang L, Chen X, Dammak H, Thi MP. Effects of Na/K evaporation on electrical properties and intrinsic defects in $Na_{0.5}K_{0.5}NbO_3$ ceramics. *Mater Chem Phys* 2009;**117**:138–41.
29. Islam MS. Ionic transport in $ABO_3$ perovskite oxides: a computer modelling tour. *J Mater Chem* 2000;**10**:1027–38.